Properties of Two Types of Calcium Channels in Clonal Pituitary Cells

D. R. MATTESON and C. M. ARMSTRONG

From the Departments of Neurosurgery and Physiology, University of Pennsylvania School of Medicine, Philadelphia, Pennsylvania 19104, and the Marine Biological Laboratory, Woods Hole, Massachusetts 02543

ABSTRACT The calcium currents of GH3 cells have been studied using the whole cell variant of the patch-clamp technique. Under conditions that eliminate sodium and potassium currents, we observed inward currents that activated within a few milliseconds, and deactivated with two time constants, ~150 μs and 3 ms at −80 mV, 18–20°C. The components are called FD and SD (fast deactivating and slow deactivating). Both components are calcium currents, and are greatly reduced when magnesium is substituted for most of the calcium in the bath. In addition to (*a*) their different rates of deactivation, the two components differ in a number of other properties. (*b*) The SD component inactivates almost completely, with a time constant of 23 ms at 20 mV, 19°C. The FD component, on the other hand, shows little or no sign of inactivation, and is almost the same in amplitude from 10 to 100 ms. The components thus seem quite independent of each other, and must arise from two independent sets of channels. (*c*) The FD channels activate more rapidly than SD at 20 mV, by a factor of ~2 as is shown in several ways. (*d*) In 10 Ca or 10 Ba, the activation curve for SD channels is ~20 mV more negative than for FD or Na channels. (*e*) FD channels conduct barium ions more effectively than calcium by a ratio of ~2. (*f*) FD channels "wash out" within minutes after the patch electrode breaks into a cell, whereas SD channel current remains relatively stable. It is argued that SD channels, because of their negative activation threshold, are involved in electrical events near threshold, and that FD channels are best suited for calcium injection once a spike has been initiated.

INTRODUCTION

Calcium channels play two major roles in the functioning of cells, serving both for electrical purposes, e.g., spike generation and pacemaking, and for the introduction of calcium into the cytoplasm, where it acts as a messenger or regulator in numerous cell functions. It is reasonable to ask whether these two major functions, and the many more specific functions they include, are served by a single type of calcium channel (cf. Hagiwara and Byerly, 1981; Llinas and Yarom, 1981). Fox and Krasne (1981) and Fishman and Spector (1981) explicitly

Address reprint requests to Dr. C. M. Armstrong, Dept. of Physiology, G4, University of Pennsylvania School of Medicine, Philadelphia, PA 19104.

J. GEN. PHYSIOL. © The Rockefeller University Press · 0022-1295/86/01/0161/22 $1.00

Volume 87 January 1986 161–182

postulated two calcium currents in, respectively, egg cells of the polychaete *Neanthes* and neuroblastoma cells. The currents were distinguishable on the basis of the voltage range over which they activate, inactivation properties, and other criteria. This was followed by the almost simultaneous description of two channels in GH3 cells (Matteson and Armstrong, 1984*a*) and in chick dorsal root ganglion (Carbone and Lux, 1984*a*, *b*), and a rush of evidence on two or more channel types in these and other tissues (Nowycky et al., 1985*a*, *b*; Tsunoo et al., 1984; Fedulova et al., 1985). The existence of more than one type of calcium channel thus seems well established, and this recognition will surely be helpful in understanding the role of calcium channels in cell functioning and in responses to hormones and drugs.

In this paper, we report in full our evidence for two calcium channel types in GH3 cells and describe their properties. Some of this work has already appeared in two short reports (Matteson and Armstrong, 1984*a*; Armstrong and Matteson, 1985).

METHODS

Culture

GH3 cells were obtained from the American Type Culture Collection. The maintenance culture was grown in 10 parts Dulbecco's modified Eagle's medium and 1 part NCTC 135 (GIBCO, Grand Island, NY), supplemented with glutamine and 5% fetal bovine serum. Once a week, the maintenance cultures were split; i.e., the cells were replated and the population was reduced by a factor of 10. The cells to be used in experiments were plated on slivers of coverslips at the time of splitting of the maintenance culture. The growth medium of both the maintenance culture and the experimental cells was replaced every second day, an essential procedure for keeping the cells in good condition.

Solutions

At the time of an experiment, a sliver of coverslip was placed in one of the protein-free external solutions given in Table I. The composition of the solutions is still evolving. We think the presence of fluoride and glutamate in the internal medium is helpful (this was not rigorously tested) and that fluoride may be important for seal formation, at least with some types of electrode glass. Outward currents in most experiments were eliminated by using cesium rather than potassium in the internal medium.

Data Acquisition

Data acquisition and pulsing were governed by a PDP 11/23 computer, which also served to subtract linear capacitive and leakage currents and to average and display data. A P/2 procedure was used in the subtraction of the capacitative and leakage currents, with control pulses usually beginning at −120 mV (Armstrong and Bezanilla, 1974).

Patch-Clamp Electronics

We used a patch clamp that generally followed the published design of Hamill et al. (1981), but which had two significant modifications. First, we used a transient cancellation circuit that generated three exponentials. The output of this circuit, as in the design of Hammill et al., fed current to the negative input of the headstage amplifier through a small capacitance. With ideal adjustment, this circuit would supply all of the current to

charge the membrane capacitance during a step, and the capacity transient would be completely eliminated from the current signal output of the patch clamp. This ideal can seldom be achieved, and the residual charging current must be drawn from the output of the headstage amplifier. This residual current passes through the feedback resistor. To improve the amplifier's ability to supply this current, it is desirable to use a relatively low-feedback resistor. We customarily used 100 MΩ. For good step performance, however, it was nonetheless essential to adjust the transient cancellation circuit carefully. We also used series resistance compensation, to compensate for the electrode resistance.

Electrodes

Following the suggestion of Dr. Jim Rae (Rae and Levis, 1984), we used Corning 8161 glass to make patch pipettes. The electrodes had a resistance of 0.5–1.2 MΩ. Step performance was gravely compromised with electrodes of higher resistance.

TABLE I

Recording Solutions

External solutions	Na*	K	Ca	Ba	Sr	Mg	Tris‡	Hepes‡
5 Ca, Tris	—	—	5§	—	—	—	158	—
5 Ba, Tris	—	—	—	5	—	—	158	—
10 Ca, Tris	—	—	10	—	—	—	150	—
10 Ba, Tris	—	—	—	10	—	—	150	—
1 Ca, 9 Mg, Tris	—	—	1	—	—	9	150	—
5 Ca, Na	138	5	5	—	—	—	—	9.5
10 Ca, Na	130	5	10	—	—	—	—	10
10 Ba, Na	130	5	—	10	—	—	—	10
10 Sr, Na	130	5	—	—	10	—	—	10
30 Ba, 0.9 Ca, Na	104	—	0.9	30	—	—	—	10

Internal solutions	Cs	Cl	F	Glu	EGTA‖	Hepes
130 CsCl, F	130	105	25	—	20	10
130 CsF, Cl	130	25	105	—	20	10
130 CsGlu, F, Cl	130	10	25	95	10	10

* In external solutions, chloride salts of all cationic species were used.

‡ External pH was adjusted to 7.35.

§ Concentrations are in millimolar.

‖ pH of internal solutions was adjusted to 7.35 by adding CsOH.

Exponential Curve Fitting

In many experiments, we fitted tail currents with the sum of two exponentials. The time constants of the two components were in all cases well separated, making it possible to get excellent fits, as judged by eye, from a simple stripping routine. The first step involved fitting a least-squares exponential to the slow component between two cursors placed well after the fast component had decayed away. This exponential was extrapolated to the beginning of the step. The fitted slow exponential was then subtracted out, and the remaining current was fitted with a least-squares exponential. The amplitude of the fast component was measured either as the initial amplitude of the fitted exponential or, if the potential for extrapolation error was large, the measured amplitude of the current remaining after subtraction of the slow exponential.

RESULTS

Two Components of Calcium Tail Current

In a previous paper, it was shown that GH3 cells have currents carried by sodium, calcium, and potassium ion (Matteson and Armstrong, 1984*b*). The work presented here concentrates on calcium currents, and our solutions were consequently designed to eliminate potassium current by using cesium ion internally, and, in most experiments, to eliminate sodium current by replacing external sodium with Tris and/or by adding tetrodotoxin. Fig. 1 shows the inward currents that flow under these circumstances, in external solutions containing 5 mM Ca, 10 mM Ba, or 30 mM Ba plus 0.9 mM Ca, for a step to 20 mV. Current during the pulse ("pulse" current) activates with a sigmoid time course and is near its maximum in a few milliseconds. Often the inward current is preceded by an outward transient of as yet unknown origin, which is evident in the 5 Ca record. The outward transient is usually larger in cells where the seal is of poor quality, and we feel that some or all of it may be an artifact of the subtraction procedure (see Methods). When the pulse terminates, the current jumps in magnitude because of the increased driving force. This is followed by a "tail" current that decays in magnitude as the channels deactivate, i.e., as their voltage-dependent activation gates close. (As shown momentarily, some of the calcium channels also "inactivate," through closing of an "inactivation gate" that is quite distinct in its properties from the activation gate.) The "tail" current decays in two phases. Two exponentials were fit to the tails by a simple stripping procedure, and the slow exponential for each tail is plotted as a continuous line. In all three solutions, the fast time constant is near 150 μs, and the slow one is more than 10 times slower, 1.8–3 ms, at 17 or 17.5°C. These two phases of decay of the tail current were our first indication of the presence of two channels.

What evidence is there that the two tail components are calcium currents? The pulse current and both components of the tail current are much smaller when magnesium is substituted for most of the external calcium, as illustrated in Fig. 2. For technical reasons, not all of the calcium can be removed from the external solution except in lucky instances: the seal between electrode and cell usually drops in resistance to unusable levels. Therefore, in the figure, 10 Ca was replaced by 1 Ca, 9 Mg. This caused a large reduction in the amplitude of pulse current, and of both components of the tail current. The reduction was reversible, and the 10 Ca trace in the figure is the average of a determination before and after immersion in 1 Ca, 9 Mg. Thus, both pulse and tail currents seem to be carried by calcium ions, for which magnesium will not substitute.

Inactivation of the Slow Tail Current

The slow component of tail current inactivates as pulse duration is increased (cf. Matteson and Armstrong, 1984*a*, *b*), while the fast component is unchanged, as illustrated in Fig. 3*A*. The figure shows activation of the current at the beginning of the pulse, and tail currents recorded after pulses of durations 7, 15, 25, 50, 75, 100, and 200 ms. The tails have both fast and slow components (cf. Fig. 1), but as the pulse is lengthened, the slow component gets progressively smaller,

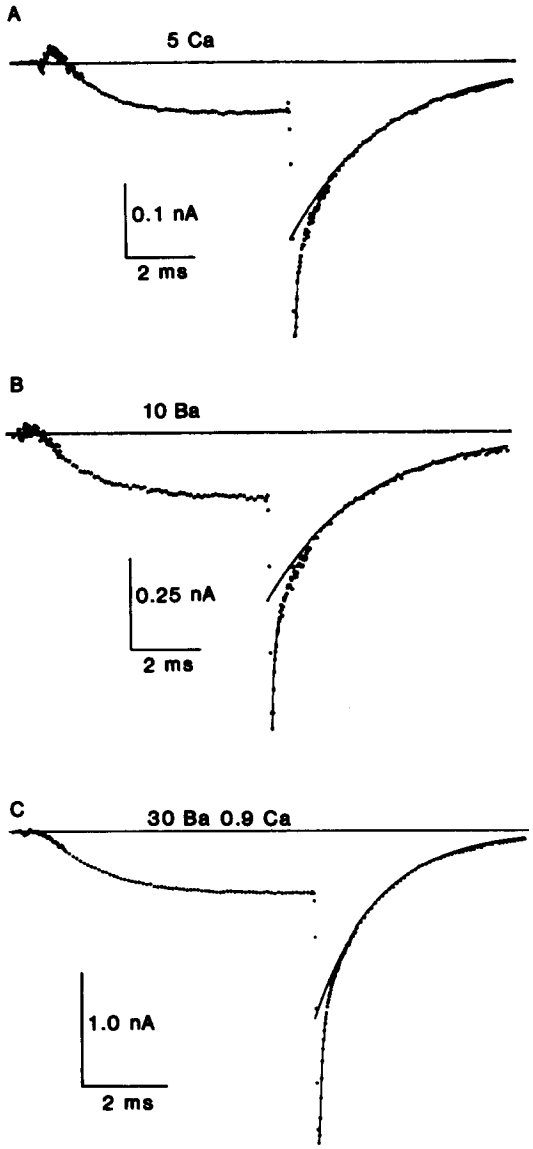

FIGURE 1. Current through calcium channels carried by calcium and barium ions. The cells were in 5 Ca (*A*), 10 Ba (*B*), or 30 Ba, 0.9 Ca (*C*). Currents are the result of a voltage step to 20 mV, with a return to the holding potential (HP) after 7 ms. The continuous curves are single exponentials fitted to the slow component of each tail. After subtracting out the slow component, the fast component was fit with a single exponential. Time constants were: (*A*) 154 μs, 2.8 ms; (*B*) 157 μs, 2.9 ms; (*C*) 123 μs, 1.8 ms. (*A*) Experiment Ap174R. 17°C. HP, −80 mV. 5 Ca, Tris//130 CsCl, F. (*B*) Experiment Ap264R. 17.5°C. HP, −80 mV. 10 Ba, Tris//130 CsCl, F. (*C*) Experiment Oc314R. 17°C. HP, −100 mV. 30 Ba, 0.9 Ca, Na, TTX//130 CsF, Cl.

with no alteration of the fast component. The tails were fit with the sum of two exponentials, and the amplitudes of the two components are plotted in Fig. 3*B*. The plot confirms one's visual impression, that the fast component is fully activated after the 7-ms pulse, and does not change significantly as pulse duration is increased up to 200 ms. The slow component is also at its maximum by 7 ms, and inactivates to a very small amplitude as the duration increases up to 200 ms. The time constants of the two components are given in the figure legend, and do not change very much as pulse duration is increased.

The two tail components behave as though they were completely independent of each other in Fig. 3 (cf. Armstrong and Matteson, 1985), which provides strong evidence that they arise from the activity of two separate sets of channels. We will name these channels SD, for slow deactivation, and FD, for fast deactivation.

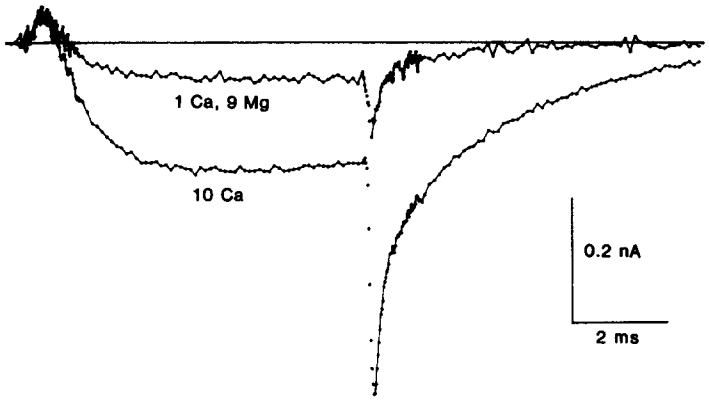

FIGURE 2. Current through calcium channels decreases on replacing calcium by magnesium. The traces shown are from a single cell, for a pulse to 20 mV with a return to −80 mV. The medium was changed from 10 Ca, Tris to 1 Ca, 9 Mg, Tris and back. In 1 Ca, 9 Mg, pulse current was decreased, together with both components of the tail current. The 10 Ca trace is the average of two records in 10 Ca, one taken before and one after immersion in 1 Ca, 9 Mg. Experiment Ap184R. 19°C. HP, −80 mV. 10 Ca, Tris or 1 Ca, 9 Mg, Tris//130 CsCl F.

Separation of Currents Using Inactivation

Inactivation of the slow component provides a convenient tool for dissecting current components. Fig. 4 shows its use for separating I_{Na} and the inactivatable component of calcium current from a record of total inward current, recorded in the absence of tetrodotoxin (TTX). The high-amplitude trace is the total current for a pulse to 20 mV, and shows during the pulse a fast transient of inward current, which decays to a plateau level of 0.146 nA. The transient component is current through TTX-sensitive Na channels and the maintained current is through calcium channels (Matteson and Armstrong, 1984*b*). The tail current has the two components described above. The trace labeled "P" is again at 20 mV, but after a 100-ms prepulse (see the pulse diagram in the figure). Most of the transient inward current is absent, and the steady current during

the pulse is reduced. The tail current after the prepulse has only the fast component.

The difference between the two traces in Fig. 4*A* is the current that is inactivated as a result of the prepulse, and this difference is plotted in Fig. 4*B*. It consists of a transient of I_{Na} and a steady current of 0.033 nA. Thus, 23% of

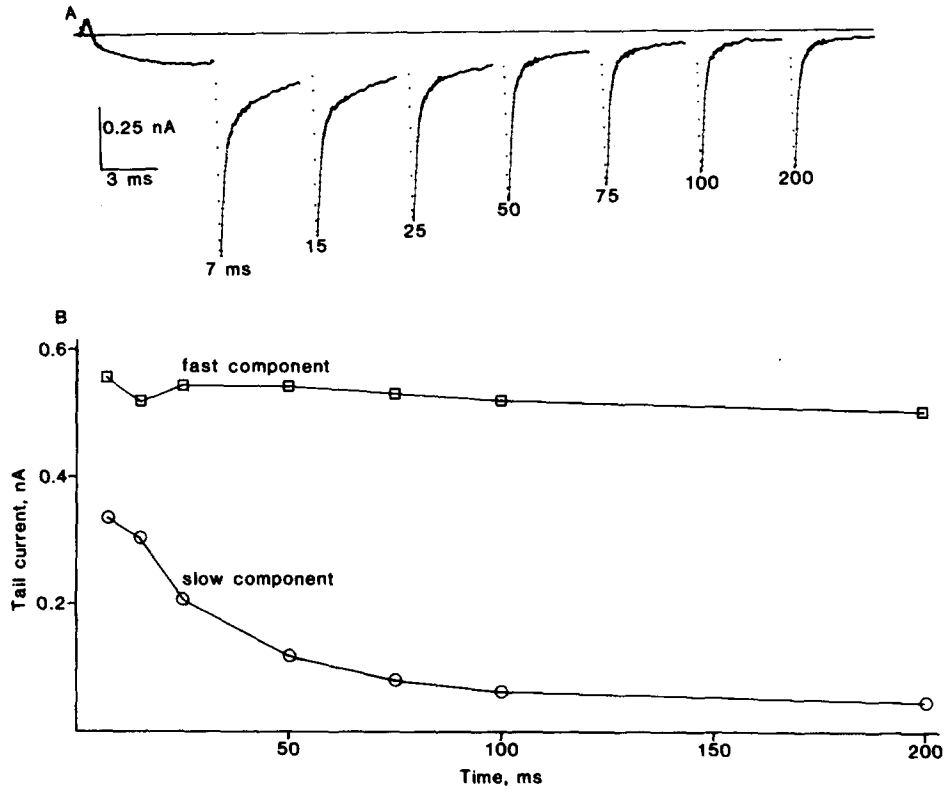

FIGURE 3. Inactivation of the slow component of the tail current. The traces shown in *A* are the current during a pulse from −80 to 20 mV, and tails recorded on returning to −80 mV after 7, 15, 25, 50, 75, 100, and 200 ms. The tails were fit with two exponentials using a simple stripping routine (see Methods). The lower curve in *B* plots the initial amplitude of the fitted slow component. After subtracting out the fitted slow component, the amplitude of the remaining current was measured and is plotted by the upper curve. The time constants for the two tail components are as follows: pulse duration: 7, 15, 25, 50, 75, 100, 200 ms; fast time constant: 255, 242, 249, 240, 240, 241, 261 μs; slow time constant: 8.4, 8.6, 9.7, 10.1, 8.8, 11.8, 12.5 ms. Experiment J1135S. 15°C. HP, −80 mV. 10 Ba, Na, TTX//130 CsCl, F.

the steady current (in this experiment) is carried through channels that inactivate. The tail current has a tiny fast component (either I_{Na} or I_{Ca}) and a slow component. In summary, inactivation affects I_{Na} as expected, some of the pulse current, and the slow component in the tail.

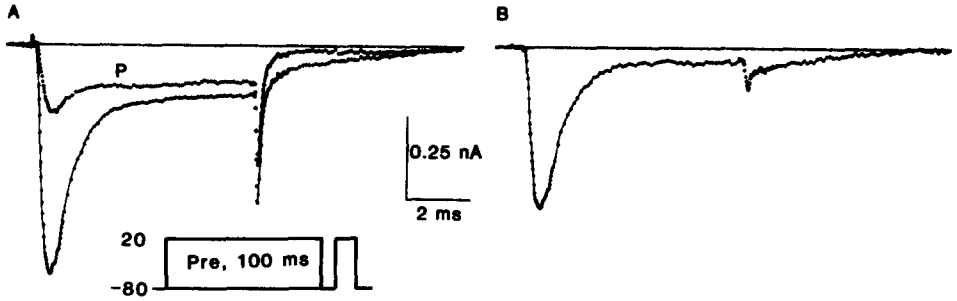

FIGURE 4. Sodium and calcium currents with and without an inactivating prepulse. (*A*) The high-amplitude trace was recorded during a test pulse to 20 mV, and on return to −80 mV. The trace labeled P was taken during a similar test pulse, but after I_{Na} and some of the calcium current had been inactivated by the prepulse shown in the pulse diagram. (*B*) This trace is the difference between the two traces in *A*, and the current is still inactivated as a result of the prepulse: I_{Na}, the slow component of the tail, and some of the maintained pulse current. Experiment Fe085R. 19.5°C. HP, −80 mV. 10 Sr, Na//130 CsGlu, F, Cl.

Separation of FD and SD Currents

In the absence of I_{Na}, the time course of the two calcium channels can be resolved during the pulse as shown in Fig. 5. The procedure was as in Fig. 4, but TTX was present to block I_{Na}. The traces in *A* are the currents at 0 mV with (P) and without a prepulse. The prepulse reduces the pulse current by more than one-third, and, as expected, almost totally eliminates the slow component of the tail. The current after the prepulse is almost entirely attributable to the FD channels, which are not subject to inactivation. The time course of activation of the SD channels can be obtained by subtracting the current after a prepulse from the total current recorded without a prepulse. This difference is plotted in part *B* of the figure, together with the current from the FD channels (trace P from *A*). It

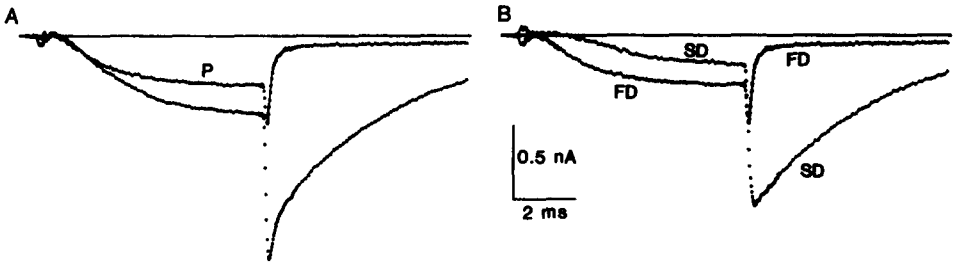

FIGURE 5. Two components of calcium current, resolved by inactivating the SD channels. The method was the same as in Fig. 4 (see legend). (*A*) The traces are test pulse current with (P) and without an inactivating prepulse. (*B*) The trace labeled FD (replotted from *A*) shows the activity of FD channels alone: the SD channels have been inactivated by the prepulse. The trace labeled SD is the difference between the two traces in *A*. It shows the activity of the SD channels, which were inactivated by the prepulse. Experiment Fe085R. 19.5°C. HP, −80 mV. 10 Sr, Na, TTX//130 CsGlu, F, Cl.

can be seen that when determined by this method, the SD channels activate more slowly than the FD channels, and deactivate much more slowly.

In Fig. 5*B* there is an apparent discrepancy in that the FD channels carry about twice as much pulse current as the SD channels, but the fast tail is much smaller than the slow one. This discrepancy disappears on fitting the fast and slow tails with exponentials and extrapolating back to the beginning of the pulse. The procedure yields time constants of 4.0 ms and 141 μs for the two components, and initial amplitudes of 2.01 (FD) and 1.22 nA (SD). The extrapolated amplitude of the fast component is thus 1.65 times larger than the slow component, which is in good agreement with the factor of 1.64 obtained from comparing the current for the SD and FD channels at the end of the pulse (FD, 0.326 nA; SD, 0.198 nA).

Activation Kinetics Determined from Tail Amplitudes

Activation of the FD and SD channels can be assayed in another way. The amplitudes of the fast and slow components after a pulse give a direct measure of the number of FD and SD channels that were activated by the time of pulse end. By varying the pulse duration and plotting the amplitudes of the two components, one can thus follow the time course of activation of the two channels. Experimental traces for this determination are shown in Fig. 6*A*, which shows, superimposed, the pulse current and the tails that follow pulses of the labeled durations. From inspection, it seems clear that the SD component grows more slowly than the pulse current, which is due to both FD and SD channels. The amplitudes of the FD and SD components are plotted in part *B* of the figure, as a function of pulse duration. From the plots, it can be seen that the FD channels activate considerably more rapidly than the SD channels, although both are almost fully activated by 3 ms. In general, the time course determined by this method is in good agreement with the one shown in Fig. 5*B*.

Voltage Dependence of the FD and SD Channels

The voltage range for activation of the two channel types can be assayed from the amplitudes of the two tail components after pulses of various amplitudes. We used pulses of 15 ms duration to assure that both FD and SD channels were fully activated and that sodium channels were inactivated, since these experiments were done in the absence of TTX. The experimental traces in Fig. 7*A* show tails after pulses to −20, 0, and 20 mV. Qualitatively, it is clear that at −20 mV the FD component is very small and is dramatically larger after pulses to 0 and 20 mV. The SD component, on the other hand, is already substantial in size at −20 mV and grows less dramatically as the voltage increases. Fig. 7*B* shows normalized plots of the FD and SD amplitudes (determined by fitting exponentials) as a function of the activating voltage, averaged from several experiments in similar but not identical solutions. The curve for the SD channels is ~20 mV to the left of the FD curve, and may be somewhat steeper. Also plotted is the curve for sodium channel activation, determined from sodium current tails after short pulses. The g_{Na} curve, like the FD curve, is well to the right of the SD curve. Thus, of the three inward current channels, the SD channels seem most likely to be involved in events near threshold.

An indication that the SD channels activate in a more negative voltage range than FD channels can also be derived from current traces during long depolarizing pulses. Fig. 8 shows current during 200-ms pulses to several voltages, recorded in 10 Ca. Virtually all of the current that is seen in the step to −20 mV inactivates; i.e. the current rises in magnitude and then falls almost to zero.

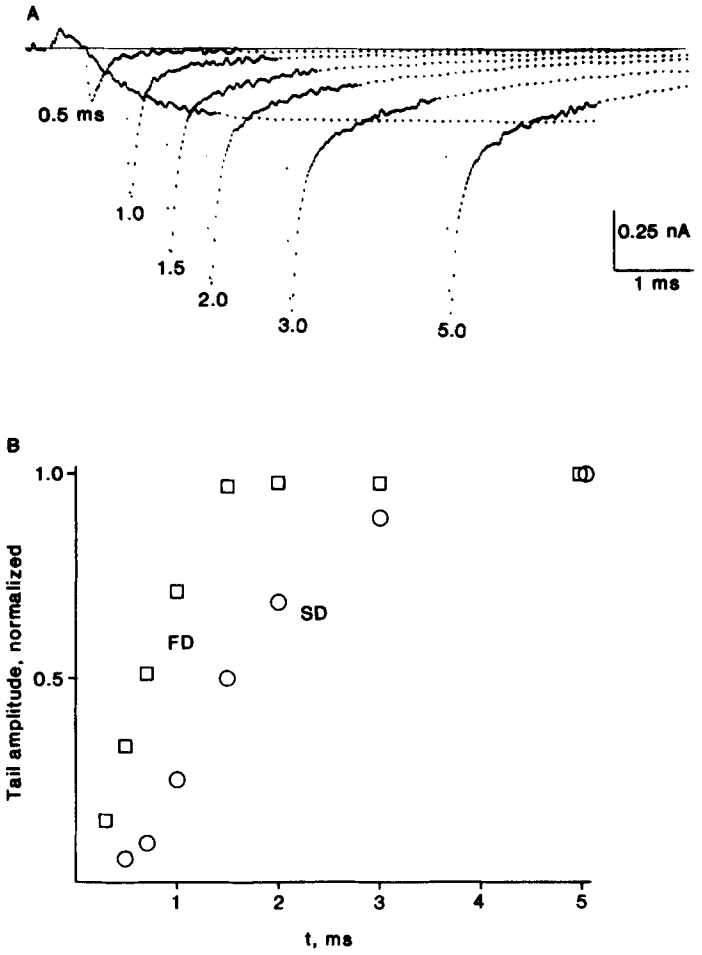

FIGURE 6. Activation kinetics of FD and SD channels determined from tail currents. (*A*) The traces show the pulse current measured at 20 mV, and tail currents at −80 mV following pulses of the indicated duration. The FD component appears to activate more rapidly than the SD component. Experiment Mr024R. (*B*) The normalized amplitudes of the FD (squares) and SD (circles) components are plotted as functions of the duration of the activating step to 20 mV. Plots are averages from four cells, and in each case the amplitudes of the fast and slow component were determined by exponential fitting. Experiments Fe294R and Mr024R. 22°C. HP, −80 mV. 5 Ba, Tris, TTX//130 CsCl, F.

Because only the SD channels inactivate, the channels open at −20 mV must be mainly SD. At 0 mV, the current inactivates with a time constant of 23 ms to 28% of its peak value, leaving a substantial residual current at pulse end. The residual current is mainly through FD channels, which are not subject to rapid inactivation, although there is a slow decline in the current amplitude that may

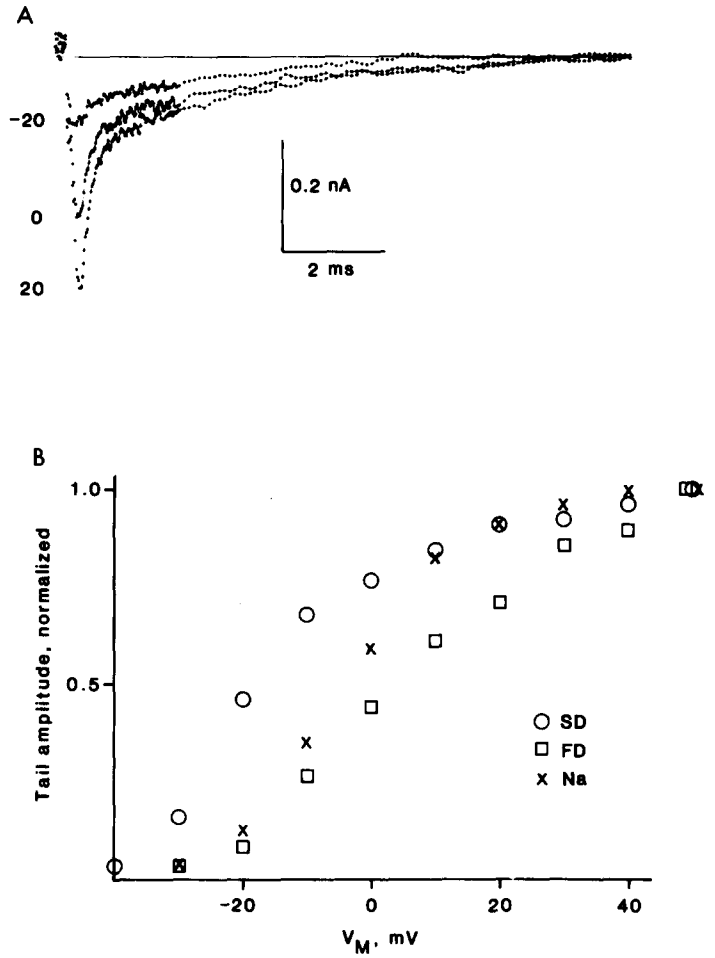

FIGURE 7. Voltage dependence of channel activation. (*A*) Tail currents following 15-ms steps to the indicated potentials. The trace at −20 mV is almost purely SD, whereas at higher voltages there is a large FD component. Experiment De213S. (*B*) Normalized amplitudes of the FD and SD components of tail current are plotted as a function of the activating potential. FD and SD amplitudes were determined by fitting two exponentials to tails like the ones in *A*. The g_{Na} curve was measured from the amplitudes of I_{Na} tails recorded after pulses too short to activate FD and SD currents. Curves were averaged from several experiments, using 5 Ca, Na or 10 Ca, Na//130 CsCl, F.

reflect slow inactivation of these channels. On repolarization to −80 mV, most of the tail current is too fast to resolve with the slow sampling used in this experiment. A small, very slow tail (time constant, 16 ms) is evident in the trace, and its origin remains to be explored. This slow tail may be related to the one in Fig. 6, where there is a very slow tail component in the trace after a prepulse.

At 20 mV, the current inactivates to 36% of its peak value, leaving more residual current than at −20 or 0 mV. The residual is again through FD channels

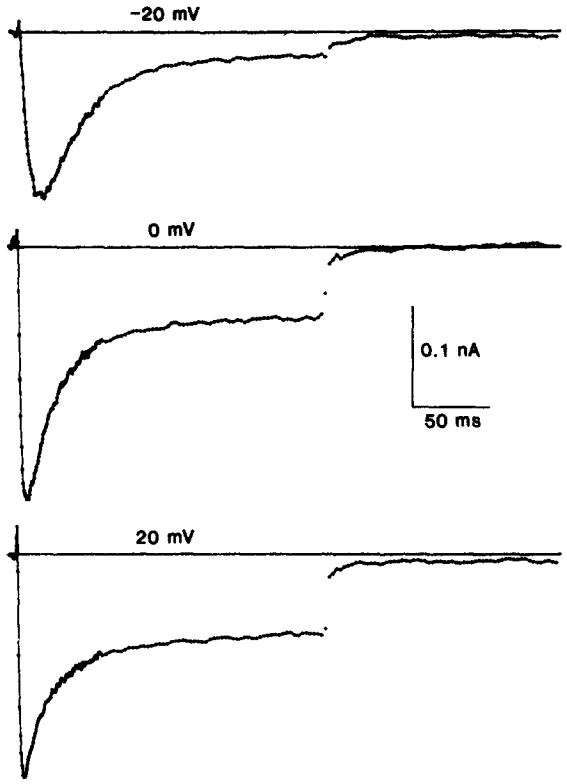

FIGURE 8. Ca channel inactivation at three voltages. The traces show 200-ms steps from −80 mV to −20, 0, and 20 mV. At −20 mV, mainly SD channels are activated. These channels inactivate almost completely, and the current at the end of the pulse is small. At higher voltages, FD as well as SD channels are activated. Since the FD channels do not inactivate, there remains a large current at pulse end. Experiment Fe125S. 19°C. HP, −80 mV. 10 Ca, Na, TTX//130 CsGlu, F, Cl.

and is larger because more of these channels are activated at 20 mV. This series of traces thus confirms that SD channels are preferentially activated by small depolarizations and that the FD channels are called into action at higher voltages.

The traces of Fig. 8 were recorded in 10 Ca, a solution that makes current through the FD channels relatively small. The result is that a large fraction of the current is carried by SD channels, which inactivate. In 10 Ba, a much smaller

fraction of the total current inactivates, because a larger fraction of the total current is through FD channels.

Recovery from Inactivation

The time course of recovery of SD channels from inactivation was measured by applying test pulses at various intervals after a 100-ms prepulse to 20 mV. The prepulse inactivated the SD channels and they recovered with time after it. The time course of recovery was approximately exponential, and the time constants are given in Table II. At 19°C, recovery has a time constant of ~0.5 s. The data are not extensive enough for us to draw conclusions about the voltage or temperature dependence of the process.

Ba/Ca Conductivity of FD and SD Channels

The ability of the two channels to conduct currents of Ca or Ba ions was tested in the experiment of Fig. 9. The initial current record from the cell was taken in 10 Ca, at a voltage of 20 mV. The medium was quickly changed to 10 Ba and

TABLE II

Time Constants of Recovery from Inactivation

Solutions	Temperature	Voltage	Time constant
	°C	*mV*	*ms*
10 Ca, Na//130 CsCl, F	16	−100	630
10 Ca, Na//130 CsCl, F	16	−100	700
10 Ca, Na//130 CsCl, F	16	−100	1,100
10 Sr, Na//130 CsGlu, F, Cl	19	−80	400
10 Sr, Na//130 CsGlu, F, Cl	19	−80	500

the illustrated trace was taken. A final record was taken on return to 10 Ca. The before and after traces in 10 Ca were very similar, and the illustrated 10 Ca trace is the average of the two. On changing from calcium to barium, the pulse current approximately doubled, the FD component of the tail increased substantially, and the SD component changed little, if at all. Exponentials were fit to the FD and SD components of the tail by a peeling procedure, and the results of the fit are given in the figure legend. The FD component was larger by a factor of 2.2 in barium.

Fig. 9*B* gives the difference between the barium and the calcium trace, and thus represents the extra current that flowed on changing to barium. It is clear that all of the extra current in the tail is flowing through FD channels, and that current through the SD channels changes little. This leads one to conclude that all of the extra pulse current is flowing through FD channels. The difference current thus gives another measure of the time course of FD channel activation and deactivation, and this measure closely resembles the FD time course shown in Fig. 5*B*, which was determined by a totally different method.

Instantaneous I-V Relation for SD Channels

The current-voltage relation for open SD channels was determined using the pulse protocol shown in Fig. 10. The channels were activated by pulse A (20

mV, 10 ms duration) and voltage was then stepped to a new level during a post-pulse. The resulting tails had both FD and SD components. The FD component was determined in isolation by performing the same procedure after a prepulse P, which inactivated the SD channels, leaving only FD current. This series of traces (FD) was subtracted from the original set (FD plus SD) to yield the SD traces illustrated in the figure. From these traces it is clear that the decay kinetics of the SD channels are voltage sensitive and progressively faster down to −100 mV.

The initial amplitudes of these traces are plotted in Fig. 10*B* as a function of voltage during the post-pulse. The curve is not linear and has a progressively shallower slope as voltage goes positive.

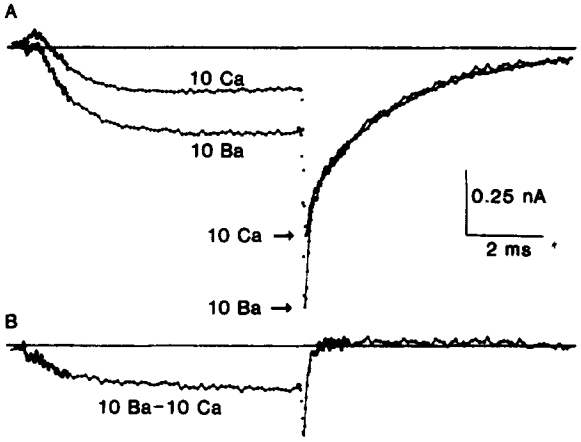

FIGURE 9. Ba/Ca conductivity of the FD and SD channels. (*A*) Currents were recorded at 20 mV with solution changes from 10 Ca to 10 Ba and back. The 10 Ca trace is the average of the records taken before and after Ba. In Ba, the pulse current and the FD component of the tail are larger. Exponentials fit to the fast and slow components gave the following amplitudes: 10 Ca: FD,0.26 nA; SD, 0.61 nA. 10 Ba: FD, 0.58 nA; SD, 0.61 nA. (*B*) The difference between the two traces in part *A* is the extra current that flows on changing to Ba. It has the time course previously determined for FD channels (e.g., Fig. 5). Experiment Ap184R. 19°C. HP, −80 mV. 10 Ca, Tris or 10 Ba, Tris//130 CsCl, F.

Similar curves were determined for the FD channels, but the potential for extrapolation error in these measurements was so large that we felt the curves were meaningless, and we have not presented them.

"Washout" Affects FD Channels

The activity of the FD channels decreases rapidly with time after the instant when the electrode breaks into the cell. An example is given in Fig. 11. The traces show total current recorded shortly after entering the cell (*A*) and 217 s

later (*C*), and the resolution of total current into FD and SD channel activity at the two times (*B* and *D*) (see figure legend for the method). Just before the end of the pulse, FD channels carry 0.38 nA of current in *A* and 0.16 nA in *C*, 217 s later. The fast component of the tail correspondingly decreases almost twofold, from 1.09 to 0.53 nA. SD channel activity declines much less, from 0.17 to 0.15 nA during the pulse (*B* and *D*), and the slow tails decrease from 1.6 to 1.4 nA.

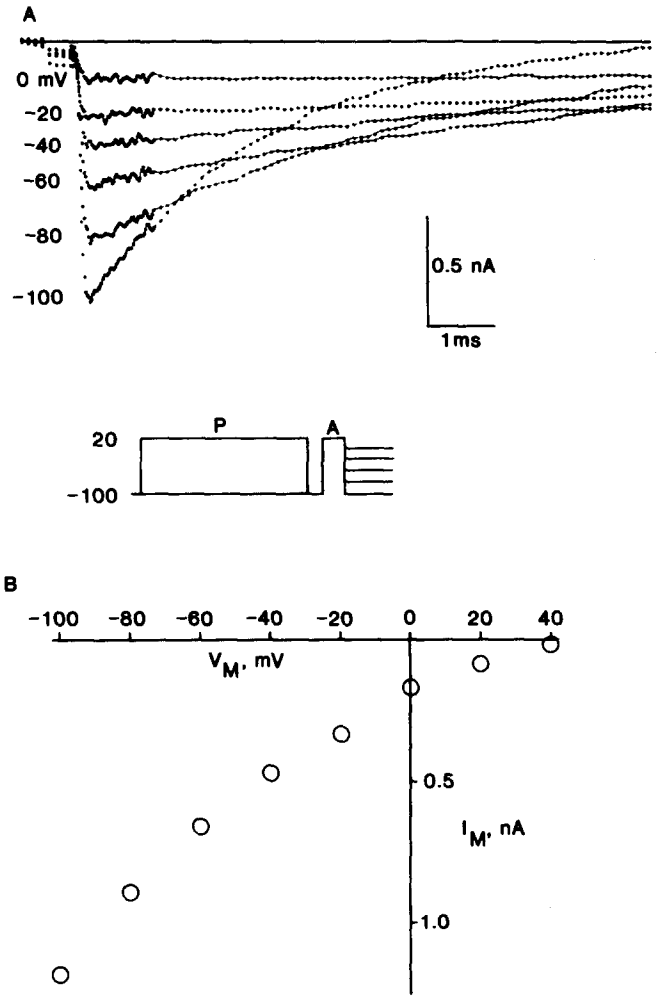

FIGURE 10. Instantaneous *I-V* relationship for SD channels. (*A*) The instantaneous currents were measured at a variety of potentials following activation of the Ca channels by a 10-ms step to +20 mV (pulse pattern in inset). Currents measured after a 150-ms prepulse to +20 mV were subtracted from those measured without a prepulse, and are plotted in the figure. (*B*) *I-V* curve. Experiment Oc314R. 13°C. HP, −100 mV. 30 Ba, 0.9 Ca, Na, TTX//130 CsF, Cl.

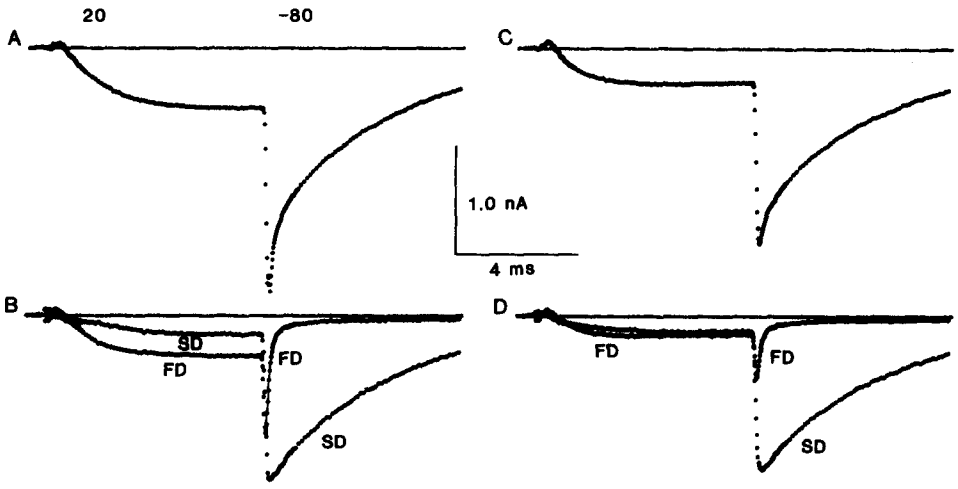

FIGURE 11. The rapid decay of FD channel activity. The traces show total current just after breaking into a cell (*A*) and 217 s later (*C*), and the resolution of total current into FD and SD channel activity just after break-in (*B*) and 217 s later (*D*). Total current is for a test pulse from −80 to 20 mV, with a return to −80 mV. For the traces labeled FD, the test pulse was preceded by a prepulse (100 ms to 20 mV, ending 5 ms before the test pulse, as in Figs. 5 and 6) to inactivate the SD channels. Trace SD is the difference between total current and trace FD. Experiment Fe085R. 19.5°C. HP, −80 mV. 10 Sr, Na, TTX//130 CsGlu, F, Cl.

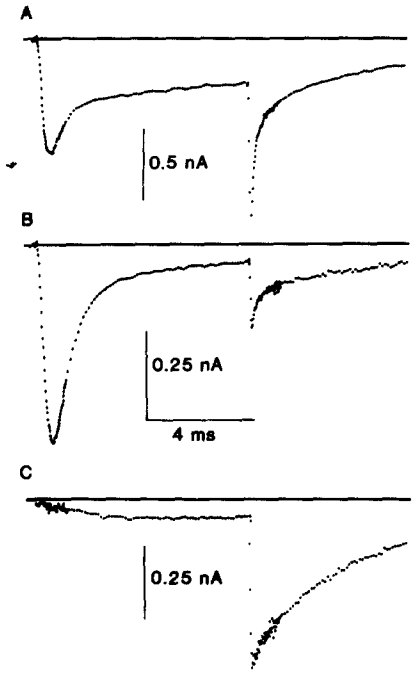

FIGURE 12. Variability of inward currents in GH3 cells. These three records of inward currents at 20 mV were recorded in identical ionic conditions. The relative amplitudes of sodium, FD, and SD currents vary widely from cell to cell. The left trace is the most commonly seen pattern, but has an unusually large FD component. HP, −80 mV. 10 Ca, Na//130 CsCl, F. (*A*) Experiment Oc094R. 18.5°C. (*B* and *C*) Experiment Oc184R. 17.5°C.

Thus, FD activity "washes out" quite quickly, and, in contrast, SD channel activity in many experiments seems quite immune to washout.

Variability of Currents

Although there is an easily recognizable "average" GH3 cell, the relative amplitudes of the three inward currents, I_{Na}, FD, and SD, vary over a wide range. Fig. 12 shows three examples of this, from three cells, all recorded at 20 mV in identical ionic conditions. The top trace is the most nearly typical pattern in the absence of TTX. There is a small sodium current during the pulse, and the tail has both FD and SD components. The FD component is larger than usual for recordings in 10 Ca. In the middle trace, sodium current is large, and the tail current has small FD and SD components. Finally, in the bottom trace, there is no indication of I_{Na} during the pulse, and the tail has only an SD component. It is interesting to note that pulse current is quite small in this cell, even though the SD component is substantial. This agrees with the preceding experiments, which show that in most cells the majority of pulse current is carried through FD channels (e.g., Fig. 5).

The cause of the variability is totally unknown and could depend on the phase of the cell cycle, or it could arise from inhomogeneity of the population or from other causes.

DISCUSSION

Two Calcium Channels in GH3 Cells

The results presented here show that there are two quite distinct components of calcium current in GH3 cells, differing from each other in at least six respects. (*a*) The time constant of deactivation is typically 150 μs for FD channels vs. ~3 ms for SD, at −80 mV and room temperature (Fig. 1). (*b*) FD channels activate more rapidly than SD channels (Figs. 5 and 6). (*c*) The SD channels inactivate almost completely, whereas the FD channels inactivate little, if at all, in 100–200 ms (Figs. 3, 5, and 8). (*d*) The activation threshold (loosely defined as the point where current though the channels becomes evident) for FD channels is about −20 mV, whereas there is appreciable SD current at −40 mV (Matteson and Armstrong, 1984*b*; Fig. 7). (*e*) The FD channels conduct Ba in preference to Ca by a ratio of ~2.2, whereas the ratio is ~1.0 for SD channels (Fig. 9). (*f*) FD channels "wash out" within a few minutes, whereas SD channel activity remains relatively stable for prolonged periods (Fig. 11).

In an earlier paper (Matteson and Armstrong, 1984*b*), we thought that the two components might reflect the activity of a single channel type with two modes of behavior, and that channels could convert from one mode to the other. With improved time resolution, it now seems clear that the two components behave independently of each other, and that interconversion from slow to fast decay is very unlikely. Perhaps the most crucial experiment is presented in Fig. 3, which shows that the FD component remains unchanged, whereas the SD component inactivates as pulse duration is increased. This experiment gives no suggestion that there is interconversion between FD and SD behavior. Instead, it strongly suggests the existence of two independent sets of channels, the FD and SD channels.

Properties of Calcium Channels in Various Preparations

There is now strong support for the idea of more than one calcium channel type in the literature, and some of the properties attributed to the channel types are

listed in Table III. The first suggestion of two channel types that we are aware of (and a somewhat tentative one) was by Hagiwara et al. (1975), who found that channels I and II differed in activation threshold, inactivation time constant, and Ba/Ca selectivity. An odd feature that does not appear in later results is that channel I current depends on the presence of external Na.

The other reports listed in the table all agree that there are two calcium channel types, and one report argues for three. Regarding the properties of the channels, there are a number of points of agreement in the table, as well as some quantitative or even qualitative disagreement that may arise from the different preparations used. First the points of agreement. (*a*) All reports agree that there are two (or more) channel types that differ in activation threshold. There is, however, a substantial difference in the activation thresholds reported. (*b*) In all reports, the low-threshold channel inactivates more rapidly and more completely. Time constants of inactivation for the low-threshold channels vary from 9 ms (10 mV, 12°C) to 35 ms (−25 mV, 20–22°C). (*c*) In three reports, the high-threshold noninactivating channel carries Ba in preference to Ca, whereas the low-threshold inactivating channel does not discriminate. (*d*) In two reports, the high-threshold channels have a more pronounced tendency to wash out. (*e*) The low-threshold channels activate within a few milliseconds at 10 or 20 mV, 12–20°C.

Points on which there is apparent disagreement, possibly owing, in some cases, to a difference in preparation or experimental conditions, are the following. (*a*) The activation threshold for the low-threshold inactivating channel varies from −75 to −40 mV. The most negative value was recorded by Fedulova et al. (1985) in 2 mM Ca, which is substantially lower than Ca in most other reports, in which higher than physiological Ca may have shifted activation to more positive voltages. (*c*) Possibly for the same reason, Fedulova et al. (1985) found a relatively negative threshold for the high-threshold channels, −55 to −50 mV vs. −6 to −20 mV in the other reports. (*d*) Fedulova et al. and possibly Carbone and Lux (1984*a*, *b*) found that high-threshold channels activate more slowly than the others. We find the opposite. (*e*) Carbone and Lux (1984*a*, *b*), working in 20 mM Ca, report that low-threshold channels have a larger single channel conductance than high-threshold channels. Nowycky et al. (1985*a*, *b*), working in 110 Ba, found the opposite. This may simply depend on the ionic conditions, 20 Ca vs. 110 Ba. (*f*) Carbone and Lux (1984*a*, *b*) found, in chick dorsal root ganglion cells, two types of calcium channels, whereas Nowycky et al. (1985*a*, *b*) found three.

There is one point that is reported only once in this group of papers, and is therefore uncontested. That is that the high-threshold channels deactivate much more rapidly than the low-threshold ones. Two time constants of deactivation were reported by Fenwick et al. (1982), 100 and 400 μs (−70 mV, room temperature), and by Lux and Brown (1984), 170 μs and 1.4 ms (−15 mV, 20°C).

Perhaps none of these findings is beyond the reach of a theoretical single channel with several modes of behavior. Such a theory would necessarily be very

TABLE III

Properties of Calcium Channels

Reference	Channel name	Preparation	$t_{1/2}$	τ_D	τ_I	V_T	Ba/Ca	γ	Washout
			ms	*ms*	*ms*	*mV*		*pS*	
Hagiwara et al. (1975)	Channel I	Starfish egg	—	—	Fast	−55 to −50	0.5 (10 mM)	—	—
	Channel II		—	—	Slow	−7 to −6	0.85 (10 mM)	—	—
Fox and Krasne (1981, 1984)	Ca I	Neanthes egg	—	—	10–50	−45	<1.0	—	—
	Ca II		—	—	Doesn't inactivate	−5 to −10	>1.0	—	—
Fishman and Spector (1981)	? Type 1	Neuroblastoma	—	—	~20 at 20–24°C	−50	—	—	—
	? Type 2		—	—	~2,000 at 20–24°C	More positive	—	—	—
Matteson and Armstrong (1984*a*, *b*)	SD	GH3 cells	1.5 at 20 mV, 22°C	3 at −80 mV, 20°C	23 at 20 mV, 19°C	−40	1.0	—	No
	FD		0.7 at 20 mV, 22°C	0.15 at −80 mV, 20°C	None in 100 ms	−20	2.2	—	Fast
Carbone and Lux (1984*a*, *b*)	LVAFI	Chick DRG	~3 at 10 mV, 12°C	—	9 at 10 mV, 12°C?	−60 to −50	—	9.5 in 20 mM Ca	—
	Usual		Slower than LVAFI?	—	Slow, incomplete	−15	—	30–40% less	—
Tsunoo et al. (1984)	? Type 1	Neuroblastoma	—	—	Fast	−50	—	—	—
	? Type 2		—	—	None in 200 ms	−20	—	—	—
Fedulova et al. (1985)	Fast	Rat DRG	1.6 at −25 mV, 20–22°C	—	35 at −25 mV, 20–22°C	−75 to −70	~1	—	No
	Slow		4 at 3 mV	—	Several hundred	−55 to −50	1.8	—	Fast
Nowycky et al. (1985*a*, *b*)	T	Chick DRG	—	—	Fast	−60	—	Tiny in 110 mM Ba	—
	L		—	—	Slow	−10	—	25 in 110 mM Ba	—
	N		—	—	Medium	? 0	—	Medium in 110 mM Ba	—

$t_{1/2}$: half-time of activation; τ_D: time constant of deactivation; τ_I: time constant of inactivation; V_T: activation threshold; Ba/Ca: conductivity ratio; γ: single channel conductance.

complex, however, and it seems most profitable to think that there is more than one channel type. The table gives one little encouragement in thinking that the channel types have identical properties in all preparations. There are, for example, substantial quantitative differences between the low-threshold inactivating channels in GH3 cells and in chick dorsal root ganglion cells. Some of these differences may become smaller when experimental conditions are made more similar, but it is not at all clear that they will disappear entirely.

Several groups agree that inactivation of the low-threshold channels is voltage dependent, and is not the result of internal Ca accumulation (Fox and Krasne, 1981, 1984; Matteson and Armstrong, 1984*b*; Fedulova et al., 1985). It would thus seem that inactivation of these channels has a different mechanism than the one found in *Paramecium* (Brehm and Eckert, 1978).

Fedulova et al. (1985) have studied the washout of the high-threshold channels and have found that it can be prevented by the addition of cAMP and MgATP. Yazejian and Byerly (1984) also report that MgATP is useful in preventing washout, but they found that cAMP is not required.

Possible Functions of Two Calcium Channel Types

In no case can it be said that the physiological function of the two (or more) calcium channel types is established, and it is perhaps worthwhile to speculate as a guide to further experiments. Calcium channels serve an electrical function in many membranes, where they are involved in spike generation and probably pacemaking. In these cases, the important element is the electrical effect of the movement of calcium across the cell membrane. Quite distinct from these purely electrical functions are the cases in which calcium injected into the cytoplasm serves as an essential signal in excitation-secretion coupling, excitation-contraction coupling, or enzyme activation.

There are reasons to believe that the two channel types we observe could be associated with these two distinct functions, SD having a primarily electrical function, and FD serving to inject calcium into the cytoplasm. The SD channels activate in a more negative voltage range than either the FD or sodium channels, and therefore seem the most likely of the inward current pathways to be involved in events near threshold. An analogous set of channels has recently been reported in squid giant axon, the so-called "threshold" sodium channels, which are said to activate ~20 mV more negative than the ordinary sodium channels (Gilly and Armstrong, 1984). GH3 cells are known to fire spontaneously, or pacemake, and it is possible that SD channels, with their negative activation range, are involved in this function. Further, SD channels have a large time constant for recovery from inactivation, and this long time constant might be the basis for pacemaking at a slow rate.

The FD channels, because of their positive activation range, seem unlikely to be important in events at threshold, and the same can be said for the sodium channels. One could also argue that the FD channels probably do not have an important electrical function, since their threshold, activation kinetics, and deactivation kinetics are all similar to the sodium channels, which, at least in many GH3 cells, carry much more current. (It has been demonstrated that Ca spikes can be generated in GH3 cells in the absence of external sodium ions

[Taraskevich and Douglas, 1980]. In pituitary cells, where FD current is larger than Na current, if such cells exist, the electrical impact of FD channels in generating spikes would be important.) On the other hand, FD channels seem well endowed to inject calcium into the cytoplasm once the decision to spike has been made by, as we postulate, the SD channels. During a spike, FD channels would activate quickly, carry a large current, and deactivate rapidly at the termination of the spike. In this regard, one can speculate that exocytosis is most effectively stimulated by a brief, intense flux of calcium, which effectively raises calcium concentration adjacent to the membrane (Simon et al., 1984).

We thank Mr. George Kleinstuber and Mr. James Falcone of Drummond Scientific Co., Broomall, PA, for redrawing the Corning 8161 glass used in our experiments.
This work was supported by National Institutes of Health grants NS12547 to C.M.A. and AM33212 to D.R.M.

Original version received 16 April 1985 and accepted version received 24 September 1985.

REFERENCES

Armstrong, C. M., and F. Bezanilla. 1974. Charge movement associated with the opening and closing of the activation gates of the Na channel. *Journal of General Physiology.* 63:533–552.

Armstrong, C. M., and D. R. Matteson. 1985. Two distinct populations of calcium channels in a clonal line of pituitary cell. *Science.* 227:65–67.

Brehm, P., and R. Eckert. 1978. Calcium entry leads to inactivation of calcium channel in *Paramecium*. *Science.* 202:1203–1206.

Carbone, E., and H. D. Lux. 1984*a*. A low voltage-activated, fully inactivating Ca channel in vertebrate sensory neurones. *Nature.* 310:501–502.

Carbone, E., and H. D. Lux. 1984*b*. A low voltage-activated calcium conductance in embryonic chick sensory neurons. *Biophysical Journal.* 46:413–418.

Fedulova, S. A., P. G. Kostyuk, and N. S. Veselovsky. 1985. Two types of calcium channels in the somatic membrane of new-born rat dorsal root ganglion neurones. *Journal of Physiology.* 359:431–446.

Fenwick, E. M., A. Marty, and E. Neher. 1982. Sodium and calcium channels in bovine chromaffin cells. *Journal of Physiology.* 331:599–635.

Fishman, M. C., and I. Spector. 1981. Potassium current suppression by quinidine reveals additional calcium currents in neuroblastoma cells. *Proceedings of the National Academy of Sciences.* 78:5245–5249.

Fox, A. P., and S. Krasne. 1981. Two calcium currents in egg cells. *Biophysical Journal.* 33:145*a*. (Abstr.)

Fox, A. P., and S. Krasne. 1984. Two calcium currents in *Neanthes arenaceodentatus* egg cell membranes. *Journal of Physiology.* 356:491–505.

Gilly, W. F., and C. M. Armstrong. 1984. Threshold channels—a novel type of sodium channel in squid giant axon. *Nature.* 309:448–450.

Hagiwara, S., and L. Byerly. 1981. Calcium channel. *Annual Review of Neuroscience.* 4:69–125.

Hagiwara, S., H. Ozawa, and O. Sand. 1975. Voltage clamp analysis of two inward current mechanisms in the egg cell membrane of a starfish. *Journal of General Physiology.* 65:617–644.

Hamill, O. P., A. Marty, E. Neher, B. Sakmann, and F. J. Sigworth. 1981. Improved patch-clamp techniques for high-resolution current recording from cells and cell-free membrane patches. *Pflügers Archiv. European Journal of Physiology.* 391:85–100.

Llinas, R., and Y. Yarom. 1981. Electrophysiology of mammalian inferior olivary neurones *in vitro*. Different types of voltage-dependent ionic conductances. *Journal of Physiology*. 315:549–567.

Lux, H. D., and A. M. Brown. 1984. Patch and whole cell calcium currents recorded simultaneously in snail neurons. *Journal of General Physiology*. 83:727–750.

Matteson, D. R., and C. M. Armstrong. 1984*a*. Evidence for two types of Ca channels in GH3 cells. *Biophysical Journal*. 45:36*a*. (Abstr.)

Matteson, D. R., and C. M. Armstrong. 1984*b*. Na and Ca channels in a transformed line of anterior pituitary cells. *Journal of General Physiology*. 83:371–394.

Nowycky, M. C., A. P. Fox, and R. W. Tsien. 1985*a*. Three types of calcium channels in chick dorsal root ganglion cells. *Biophysical Journal*. 47:67*a*. (Abstr.)

Nowycky, M. C., A. P. Fox, and R. W. Tsien. 1985*b*. Multiple types of calcium channel in dorsal root ganglion cells distinguished by sensitivity to cadmium and single channel properties. *Neuroscience Abstracts*. 10:526.

Rae, J. L., and R. A. Levis. 1984. Patch voltage clamp of lens epithelial cells: theory and practice. *Molecular Physiology*. 6:115–162.

Simon, S. M., M. Sugimori, and R. Llinas. 1984. Modeling of submembranous calcium-concentration changes and their relation to rate of presynaptic transmitter release in the squid giant synapse. *Biophysical Journal*. 45:264*a*. (Abstr.)

Taraskevich, P. S., and W. W. Douglas. 1980. Electrical behaviour in a line of anterior pituitary cells (GH cells) and the influence of the hypothalamic peptide, thyrotrophin releasing factor. *Neuroscience*. 5:421–431.

Tsunoo, A., M. Yoshii, and T. Narahashi. 1984. Two types of calcium channels in neuroblastoma cells and their sensitivites to cyclic AMP. *Neuroscience Abstracts*. 10:527.

Yazejian, B., and L. Byerly. 1984. Temporary reversal of calcium current washout in internally perfused snail neurons. *Biophysical Journal*. 45:37*a*. (Abstr.)